



PREDICTION OF BUOYANT, TURBULENT FLOW BY A LOW-REYNOLDS-NUMBER k - ϵ MODEL

Q. Chen, Ph.D.

Associate Member ASHRAE

A. Moser, Ph.D.

Member ASHRAE

A. Huber

ABSTRACT

A low-Reynolds-number k - ϵ model of turbulence was used for the prediction of natural convection flow in cavities with Rayleigh numbers on the order of 10^{10} . The Boussinesq approximation was used for buoyancy, and the buoyancy production terms in the k and ϵ equations were also studied.

The results indicate that the computed velocity and temperature profiles and convective heat exchanges by the model are in rather good agreement with the measurements. The influence of the buoyancy production is small on velocity and temperature profiles but is considerably large on the kinetic energy profiles. For the indoor airflow computation, use of the low-Reynolds-number model with buoyancy production terms is recommended so that correct indoor air velocity fields, air temperature distributions, convective heat transfer coefficients, and comfort parameters can be obtained.

INTRODUCTION

There are numerous practical flow problems related to buildings that can be solved profitably by numerical techniques. A successful numerical model would be an ideal tool to help a researcher understand the complex phenomena of flow problems and help a designer choose the optimum design from a number of possible alternatives. The study of air flow in rooms using numerical calculation techniques has been done for nearly 20 years and has achieved some successes, as reviewed by Kumar (1983) and Whittle (1986). Recently, more publications concerning this problem have become available, such as SAAHI (1987), Chen et al. (1988), Murakami et al. (1988), and a special issue of a trade magazine (*Building and Environment* 1989). The range of airflow simulations, which originally comprised laminar, one- and two-dimensional, steady, and isothermal situations, has been enlarged to include turbulent, three-dimensional, transient, and buoyancy-affected flows. Recent results (*Building and Environment* 1989) indicate that the k - ϵ model of turbulence

(Launder and Spalding 1974) is still the most appropriate model for practical flow applications. The set of model equations is suitable for high-Reynolds-number flow. For wall flow, where local Reynolds numbers are very low, the equations are normally used in conjunction with empirical wall function formulas. The success of this method depends on the "universality" of the turbulent structure near the wall. When disagreements are found between measurements and predictions, it is difficult to judge whether the weakness of the method lies in the basic model equations or in the wall function formulas.

When the wall functions are used, the first grid in the numerical solution has to be sufficiently remote from the wall for (k^2/ν) to be much greater than unity—so much greater, in fact, that the viscous effects are entirely overwhelmed there by the turbulent ones. This may result in some of the grids being located in the outer region of the velocity profile, as shown in Figure 1. The logarithmic wall function (Launder and Spalding 1974), which is widely used today, can still yield rather good results for fully developed, zero-pressure-gradient boundary layers in the outer region. However, Hammond (1982) showed that the velocity profile for a plane wall jet is very different from that at the zero-pressure gradient in the outer region, and the logarithmic wall function is invalid there without any modifications. The boundary velocity profile of air flow in a room may be located somewhere between that of the zero-pressure gradient and that of the plane wall jet. Hence, the wall function can hardly present good results for the air flow near walls in a room (Chen 1988). On the other hand, Chen (1988) also reported that air flows in rooms, in many cases, include natural or mixed convection, and the overall turbulence Reynolds numbers (R_t) are rather small. The high-Reynolds-number k - ϵ model of turbulence with the logarithmic wall functions may not be suitable for use both near the wall and far away from it. Therefore, it is necessary to apply an appropriate low-Reynolds-number model of turbulence for the computations of indoor airflow patterns.

Qingyan Chen is a research scientist; Alfred Moser, a staff scientist; and Arthur Huber, a research assistant at the Energy Systems Laboratory, Swiss Federal Institute of Technology, ETH-Zentrum, Zurich, Switzerland.

THIS PREPRINT IS FOR DISCUSSION PURPOSES ONLY, FOR INCLUSION IN ASHRAE TRANSACTIONS 1990, V. 96, Pt. 1. Not to be reprinted in whole or in part without written permission of the American Society of Heating, Refrigerating and Air-Conditioning Engineers, Inc., 1791 Tullie Circle, NE, Atlanta, GA 30329. Opinions, findings, conclusions, or recommendations expressed in this paper are those of the author(s) and do not necessarily reflect the views of ASHRAE.

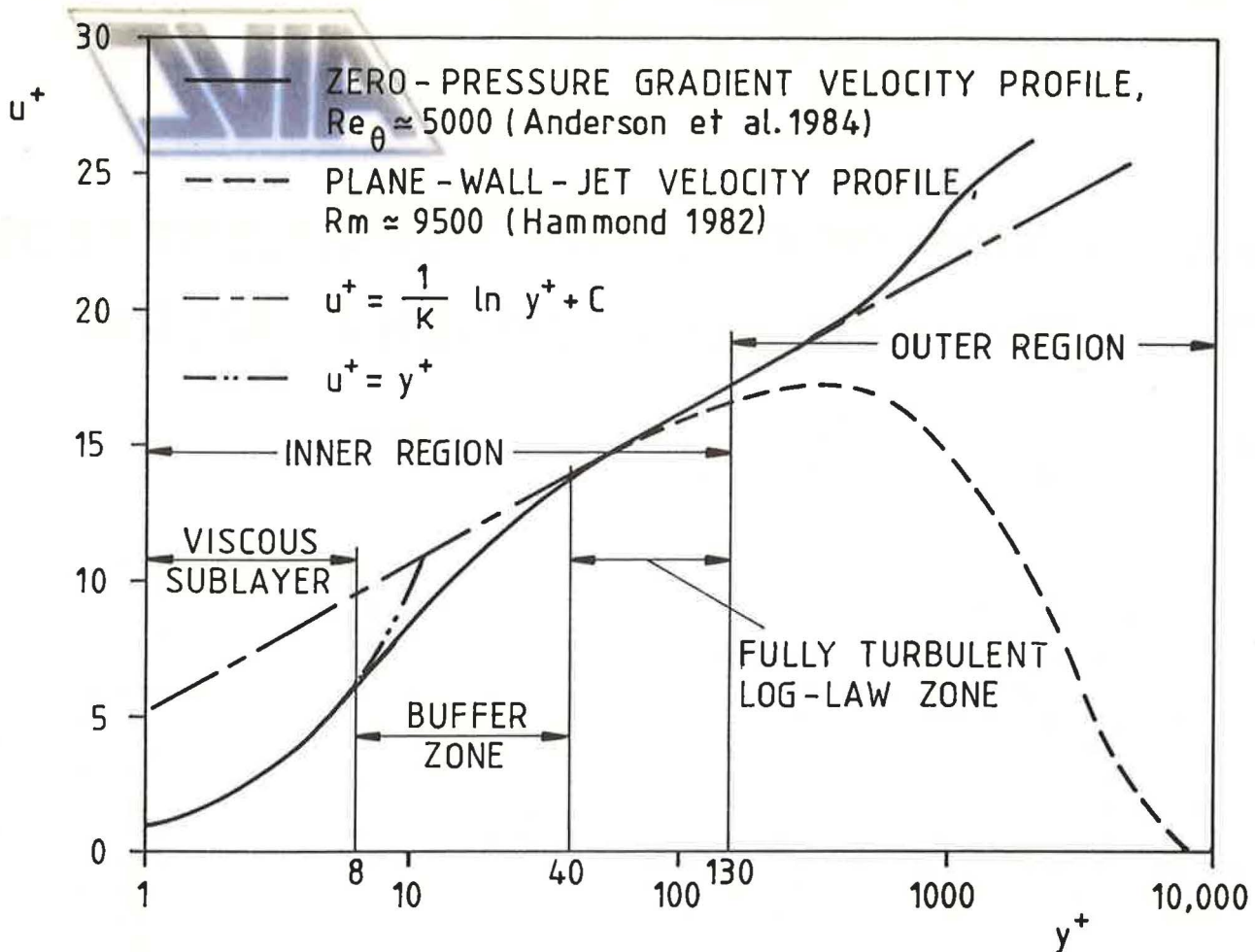


Figure 1 Velocity profiles in the turbulent boundary layer over a smooth flat plate

Some studies concerning the application of low-Reynolds-number models for natural or mixed convection in a cavity have been conducted in the past few years (e.g., Humphrey and To [1986]; Betts and Dafa'Alla [1986]). The foregoing studies were for natural or mixed convection with a relatively low Rayleigh number (up to 10^9). Few validations of low-Reynolds-number models were performed for Rayleigh numbers greater than 10^{10} , which is a typical value in a room with natural or mixed convection.

In addition to the low-Reynolds-number property, buoyancy is the main factor in natural convection. For mixed convection, buoyancy is also one of the dominant factors for indoor airflow problems. Because the insulation of buildings has been improved in order to reduce heat loss in winter and heat gain in summer, there can be a reduction of air supply, since the space load becomes smaller. Such a reduction, in many cases, generates a non-uniform distribution of indoor air temperature that is also influenced by the heat transfer through walls and windows and heat generation by room occupants or heaters, etc. Besides the buoyancy term in the momentum equation, the buoyancy production terms in the equations of turbulence energy and turbulence dissipation rate also interact with the transportation of momentum and energy. Hence, it is also necessary to study the influence of the buoyancy production terms in the equations of the kinetic energy of

turbulence (k) and the dissipation rate of turbulence energy (ϵ) on indoor airflow patterns.

As we know, the air velocity, air temperature, and turbulence energy distributions within a room are related to comfort, and the convective heat transfer coefficient for a wall is one of the basic parameters used for space load calculation and the analysis of building energy consumption. If they are computed by an airflow program, it is necessary to apply an appropriate low-Reynolds-number model of turbulence, as previously mentioned. Hence, to find a suitable low-Reynolds-number model will be the main subject of this work.

OUTLINE OF THE TURBULENCE MODEL

The turbulence model used will be described in two parts. The first part concerns the Lam-Bremhorst k - ϵ model for low Reynolds numbers, and the second deals with the buoyancy production term in the k and ϵ equations.

The Lam-Bremhorst k - ϵ Model of Low Reynolds Number

Many suggestions have been made over the past few years for the extension of turbulence closure models to enable their use at low Reynolds numbers and to describe the flow close to a solid wall. Most of the extended models incorporate either a wall damping effect, a direct effect of

molecular viscosity, or both, on the empirical constants and functions in the turbulence-transport equations devised originally for the high-Reynolds-number, fully turbulent flows remote from the walls. In the absence of reliable turbulence data in the immediate vicinity of a wall or at low Reynolds numbers, these modifications have been based largely upon comparisons between calculations and experiments in terms of global parameters. Patel et al. (1985) reviewed the existing two-equation, low-Reynolds-number turbulence models with a systematic evaluation. They found that most modifications to basic high-Reynolds-number turbulence models lack a sound physical basis. The results of each of the models were compared for different flows, and it was not clear which of the many proposed models could be used with confidence. From an overall examination of the results, they concluded that the models of Launder and Sharma (1974), Chien (1982), and Lam and Bremhorst (1981), which are based on the k - ϵ model, and that of Wilcox and Rubesin (1980) yield comparable results and perform considerably better than the others. However, Patel et al. (1985) also suggest that even these need further refinement if they are to be used with confidence to calculate near-wall and low-Reynolds-number flows. Further, Betts and Dafa'Alla (1986) studied the buoyant, turbulent air flow in a tall rectangular cavity with a Rayleigh number of 0.81×10^6 by the same turbulence models of low Reynolds number used by Patel et al. (1985). Their results showed that only the models of Launder and Sharma (1974) and Hassid and Poreh (1978) were reasonably comparable with their experimental data, but none of them was very satisfactory. In addition, they were unable to obtain converged results with the model of Lam and Bremhorst (1981).

As already mentioned, the k - ϵ model is generally used for airflow simulations in and around buildings. The model of Lam and Bremhorst (1981), which is based on the k - ϵ model, modifies the direct effect of molecular viscosity. The construction of the model can be done very easily in most existing computer programs that use the high-Reynolds-number k - ϵ model. This model gave rather good results in the studies of Patel et al. (1985) and was not well tested by Betts and Dafa'Alla (1986). Therefore, this model was selected in the present research for predicting low-Reynolds-number flows in cavities with Rayleigh numbers greater than 10^{10} .

In the model of Lam and Bremhorst, the transport equations of the kinetic energy (k) and the dissipation rate of turbulence energy (ϵ) are determined from:

$$\frac{Dk}{Dt} = \frac{\partial}{\partial x_j} \left[\left(\frac{\nu_t}{\sigma_k} + \nu_l \right) \frac{\partial k}{\partial x_j} \right] + \nu_t \left(\frac{\partial V_i}{\partial x_j} + \frac{\partial V_j}{\partial x_i} \right) \frac{\partial V_i}{\partial x_j} - \epsilon \quad (1)$$

$$\frac{D\epsilon}{Dt} = \frac{\partial}{\partial x_j} \left[\left(\frac{\nu_t}{\sigma_\epsilon} + \nu_l \right) \frac{\partial \epsilon}{\partial x_j} \right] + C_1 f_1 \nu_t \frac{\epsilon}{k} \left(\frac{\partial V_i}{\partial x_j} + \frac{\partial V_j}{\partial x_i} \right) \frac{\partial V_i}{\partial x_j} - C_2 f_2 \frac{\epsilon^2}{k} \quad (2)$$

The time-averaged flow field can be determined through the eddy viscosity given by:

$$\nu_t = C_\mu f_\mu k^2 / \epsilon \quad (3)$$

where

$$\begin{aligned} \sigma_k &= 1.0 \\ \sigma_\epsilon &= 1.3 \\ C_1 &= 1.44 \\ C_2 &= 1.92 \\ C_\mu &= 0.09 \end{aligned}$$

In fact, these equations are a general form of those given by Launder and Spalding (1974) in which the functions f_1 , f_2 , and f_μ are all assumed to be identically one. This assumption cannot be valid within a laminar sublayer or in low-Reynolds-number flows. The functions f_μ , f_1 , and f_2 are given by the following equations:

$$f_\mu = (1 - e^{-A_\mu R_k})^2 \left[1 + \frac{A_l}{R_l} \right] \quad (4)$$

$$f_1 = 1 + \left[\frac{A_{C1}}{f_\mu} \right]^3 \quad (5)$$

$$f_2 = 1 - e^{-R_l^2} \quad (6)$$

where the turbulence model constants are $A_\mu = 0.0165$, $A_l = 20.5$, and $A_{C1} = 0.05$, and R_k and R_l are turbulence Reynolds numbers.

The Buoyancy Production Terms in the k and ϵ Equations

Since the temperature difference in room air is relatively small, it is common practice to use the Boussinesq approximation. This approximation takes air density as constant and considers buoyancy influence on air movement in the momentum equation via the following term:

$$-\beta(T - T_o)g_i \quad (7)$$

Since the k and ϵ equations are derived from the momentum equation, the buoyancy term in the momentum equation is then changed into buoyancy production terms in the k and ϵ equations. The buoyancy production term for the k equation is:

$$S_k = -\frac{\beta}{C_p} \overline{V_i H'} g_i \quad (8)$$

where H is enthalpy. This term can be approximated as:

$$S_k = -\frac{\beta}{C_p} \overline{V_i H'} g_i = \beta \frac{\mu_t}{\rho \sigma_H} \frac{\partial(T - T_o)}{\partial x_i} g_i \quad (9)$$

S_k is an additional source term on the right side of Equation 1 (Nielsen et al. 1979). A similar method can be applied to the ϵ equation to generate:

$$S_\epsilon = -2 \frac{\mu_t}{\rho} \frac{\partial V_i}{\partial x_j} \frac{\partial H'}{\partial x_j} = C_3 \frac{\epsilon}{k} S_k \quad (10)$$

where $C_3 = 1.44$. Equations 9 and 10 are the additional terms in the right side of Equations 1 and 2, respectively.

The Boundary Conditions

When a low-Reynolds-number k - ϵ model is applied, no wall function formulas are required because the model is valid for the whole flow domain. However, the boundary conditions for k and ϵ must be specified. We have tested a number of methods as reviewed by Patel et al. (1985), but it is very difficult to obtain converged and correct results. Only the following two methods present good results.

The first one is recommended by Parry (1989), where a zero value is assigned at the wall for the k equation and

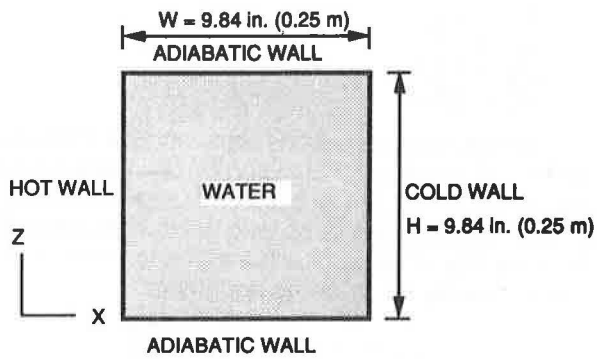


Figure 2 Sketch of the small-scale water-filled cavity

$$\epsilon = \frac{2\nu k}{y^2} \quad (11)$$

for the ϵ equation for the grid cell close to the wall.

The wall function formulas are still used as the second method, but the distance between the wall and the first grid can be very small. This indicates that the first grid points will be located inside the viscous layer. In this circumstance, the second grid points may still be in the inner region of the boundary layer and the low-Reynolds-number model will work well for those points. In the inside viscous layer, the wall function formulas present linear velocity and temperature distributions, and they can be accepted for air flow in a room. This is different from the application of the high-Reynolds-number model with the wall function formulas in which the first grid must be sufficiently remote from the wall.

VALIDATION OF THE TURBULENCE MODEL

Numerical Solution

A computer code developed by Rosten and Spalding (1987) was extended to include the turbulence model formulations described above. The computational method involves the solution, in finite-volume form, of two- or three-dimensional conservation of mass, momentum, energy, turbulence energy, and the dissipation rate of turbulence.

The methodology for performing the numerical calculations uses under-relaxation and false time step factors for obtaining a convergent solution. All calculations were performed using an upwind differencing scheme and "staggered grids." For the present study, a non-uniform grid is used to produce a very fine grid near the boundary and a coarse grid in the central region of the flow field. The grid for the two-dimensional cases is 53×53 and will be described in the following sections. A detailed description of the mathematical model and solving procedure is given by Chen (1988).

Validation of the Model in a Small-Scale Water-Filled Cavity

Aside from its intrinsic value, the accurate modeling of turbulent natural convection for a cavity with a hot wall and a cold wall is considered to be a logical first step toward the numerical simulations of more complex, buoyancy-affected, turbulent flows related to buildings. However, in reviewing the literature, it becomes apparent that even the case of steady, two-dimensional natural convection with turbulent flow in a cavity has not yet been satisfactorily

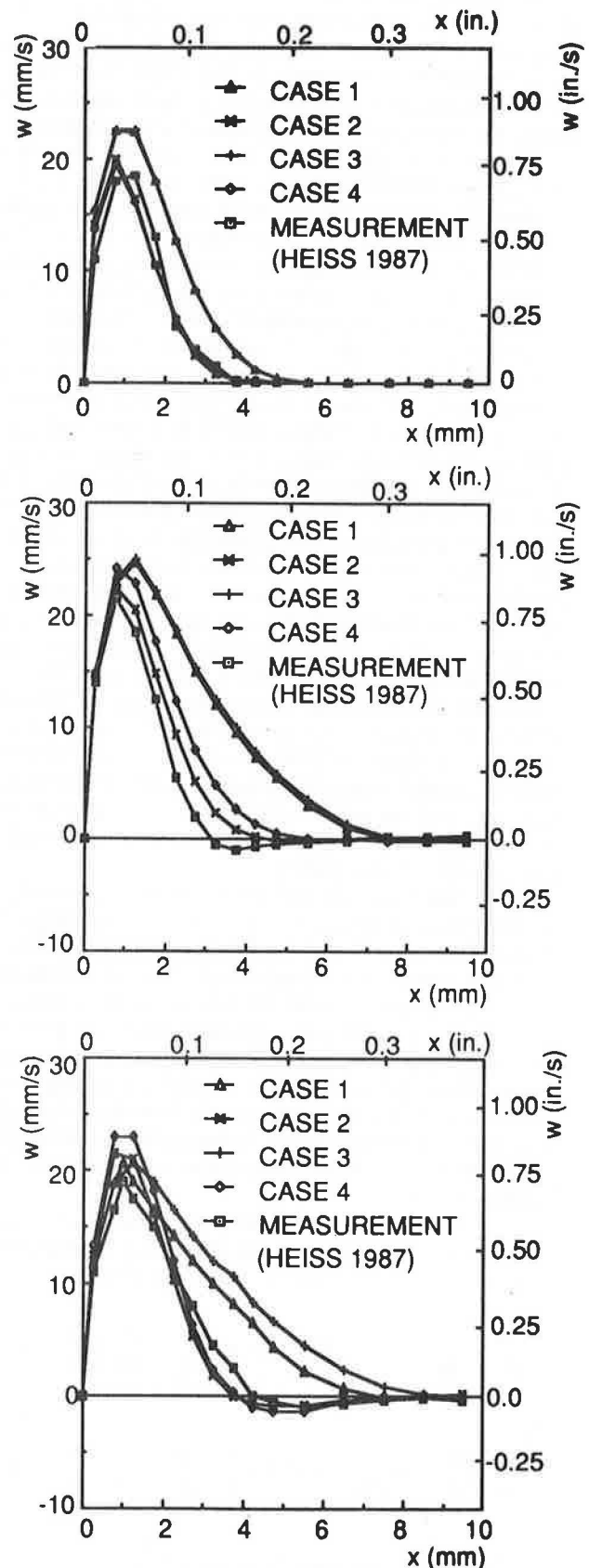


Figure 3 Profiles of vertical component of velocity near the hot wall in different heights (top figure for the section $z = 2.56$ in. [65 mm], middle for $z = 4.92$ in. [125 mm], and bottom for $z = 7.36$ in. [187.5 mm])

TABLE 1
Model Used in the Four Cases

Case No.	High-Reynolds-number model	Low-Reynolds-number model	Buoyancy production terms in k and ϵ equation
1	Yes	No	No
2	No	Yes	No
3	Yes	No	Yes
4	No	Yes	Yes

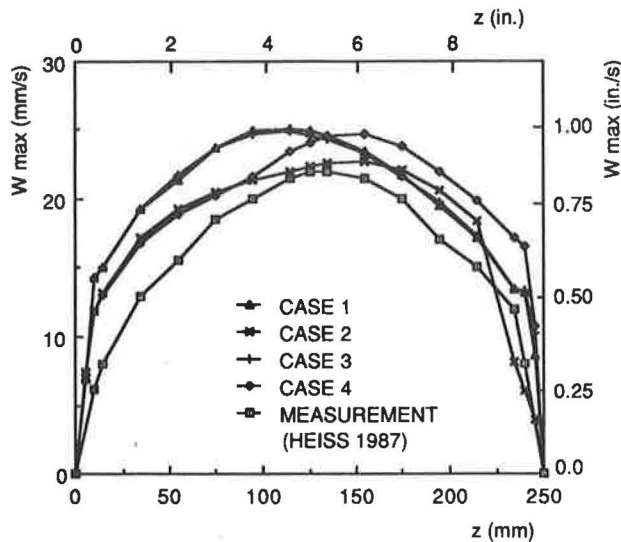


Figure 4 Relationship between the maximum vertical component of velocity (w) and the cavity height

resolved. Therefore, the validation of the turbulence model is first carried out for a two-dimensional square cavity, as shown in Figure 2, for which detailed measurements are available (Heiss 1987).

This square cavity is 9.84 in. (250 mm) in width and height and the flow is controlled to be two-dimensional. In order to simulate the air flow in a room, the Rayleigh number of the cavity was modeled to be similar to that of a full-scale room. Hence, the medium used in the cavity was water instead of air. The cavity was heated by one of the side walls and cooled by the other. The temperature difference between the two side walls was 78.1°F (43.4°C). The top and bottom walls were controlled to be adiabatic. The mean temperature of the water was 102.2°F (39.0°C). The corresponding Rayleigh number is 2.5×10^{10} .

In order to study the low-Reynolds-number model and the buoyancy production terms in the k and ϵ equations, the computations were performed for four cases, as shown in Table 1.

The calculated profiles of the vertical component of velocity (w) near the hot wall in different heights (different z sections) for the four cases and the corresponding measured results (Heiss 1987) are given in Figure 3. The velocity profiles computed by applying the low-Reynolds-number k - ϵ model (Cases 2 and 4) are in good agreement with the measurements. The profiles calculated by the high-Reynolds-number k - ϵ model (Cases 1 and 3) deviate from the measurements. We define a maximum error between the computations and the measurements in the velocity profiles as:

$$e_{\max}(z) = \max \left| \frac{W_{\text{computed}} - W_{\text{measured}}}{W_{\max, \text{measured}}} \right| \times 100\% \quad (12)$$

where $W_{\max, \text{measured}}$ is the peak value of the velocity (w) in the profile. The e_{\max} in section $z = 7.36$ in. (187.5 mm) for Case 3, which uses the high-Reynolds-number model with buoyancy production terms in k and ϵ equations, can be as large as about 61%. This means that if the high-Reynolds-number model is applied for the airflow computation in a room, it may result in very significant errors in the predicted velocity field.

The influence of the buoyancy production terms in the k and ϵ equations is not very significant. From the computations, it seems that the introduction of the buoyancy production terms (Cases 3 and 4) results in a slight discrepancy.

It should be pointed out that the low-Reynolds-number model (Cases 2 and 4) still gives a too-high peak value for w velocity profiles. Figure 4 shows the maximum w velocity distribution in relation to the height of the wall. Among these four cases, the low-Reynolds-number model without buoyancy production terms in the k and ϵ equations (Case 2) presents the best results.

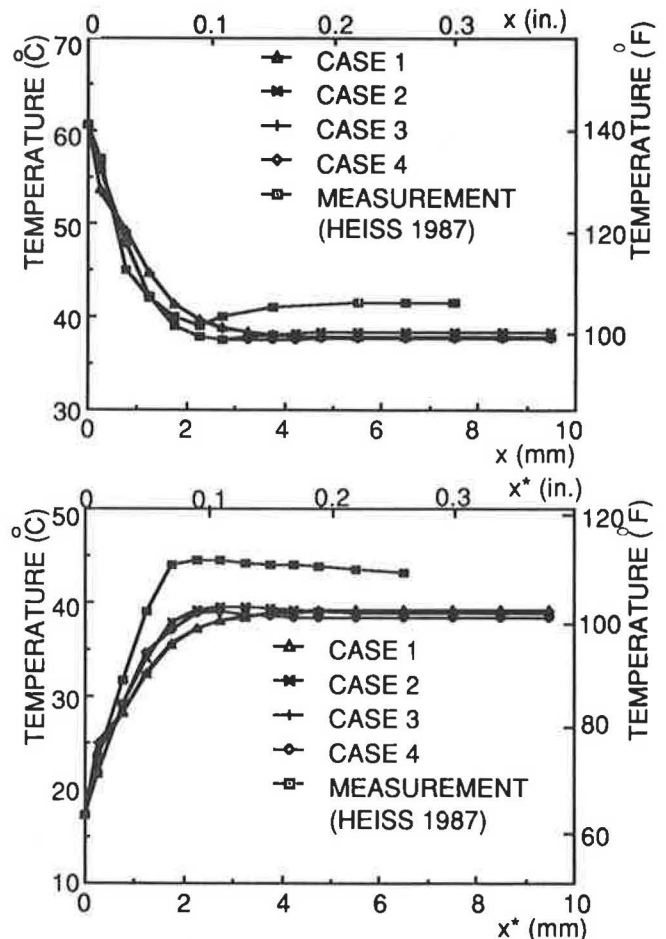


Figure 5 Temperature profiles (top figure for near the hot wall in the section $z = 4.41$ in. [112 mm], bottom for near the cold wall in the section $z = 5.43$ in. [138 mm], where x^* is the distance to the cold wall)

The near-wall temperature profiles for the hot and cold walls are illustrated in Figure 5. The computations for the four cases show similar results, and the temperatures far

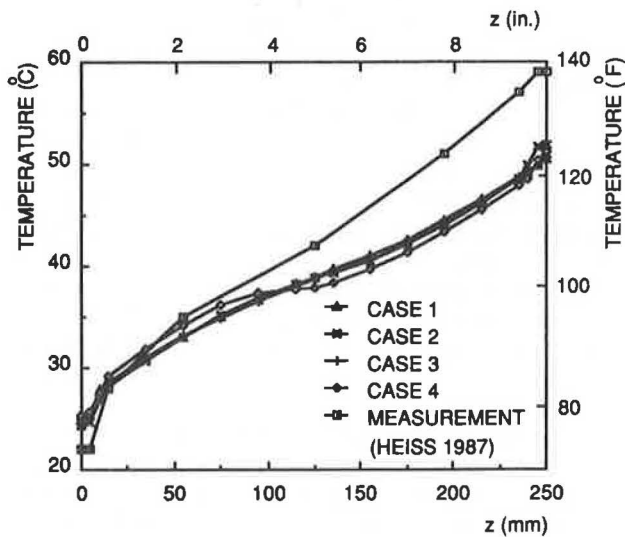


Figure 6 Vertical temperature profiles in the middle section $x = 4.92$ in. (125 mm)

from the wall in all four cases are lower than those in the measurement. Figure 6 shows the vertical temperature distribution in the section $x = 4.92$ in. (125 mm) (the middle section).

It seems the overall temperature in the cavity of the measurement is higher than that of the computations. In the computations, all the water physics properties are assumed to be temperature independent. If the medium is air, this assumption is acceptable. With this assumption, the flow and temperature distributions are always symmetrical to the center point of the cavity. However, the thermal conductivity of water is $0.343 \text{ Btu/h}\cdot\text{ft}\cdot^\circ\text{F}$ ($0.595 \text{ W/m}\cdot\text{K}$) when the water temperature is 63°F (17.3°C) but $0.376 \text{ Btu/h}\cdot\text{ft}\cdot^\circ\text{F}$ ($0.651 \text{ W/m}\cdot\text{K}$) when the temperature is 141°F (61.7°C). The laminar kinetic viscosity of water is decreased from $1.16 \times 10^{-5} \text{ ft}^2/\text{s}$ ($1.077 \times 10^{-6} \text{ m}^2/\text{s}$) to $0.50 \times 10^{-5} \text{ ft}^2/\text{s}$ ($0.463 \times 10^{-6} \text{ m}^2/\text{s}$) in this temperature range. In the viscous sublayer, the heat transfer flux is proportional to the thermal conductivity and is inversely proportional to the laminar kinetic viscosity. This means that with the same temperature differences, the heat gain from the hot wall is larger than the heat loss to the cold wall. In the steady state, the temperature difference between the hot wall and the cavity center should be smaller than that between the cavity center and the cold wall in order to maintain the energy balance. As a result, the average water temperature in the cavity is higher than the mean temperature of the hot and cold walls. This can be the main reason for the discrepancy between the computations and the experiment in the temperature distribution.

Although the temperature profiles calculated in the four cases look similar, the heat fluxes are not the same. The heat gain from the hot wall (or the heat loss to the cold wall) is $5601 \text{ Btu/h}\cdot\text{ft}$ (5382 W/m) for Case 1, $3578 \text{ Btu/h}\cdot\text{ft}$ (3438 W/m) for Case 2, $5597 \text{ Btu/h}\cdot\text{ft}$ (5379 W/m) for Case 3, and $3524 \text{ Btu/h}\cdot\text{ft}$ (3386 W/m) for Case 4. The accounting for the buoyancy production terms in the k and ϵ equations (Cases 3 and 4) does not have a significant influence on the heat transfer. But the difference of the heat fluxes by the high- and low-Reynolds-number k - ϵ models is great. For

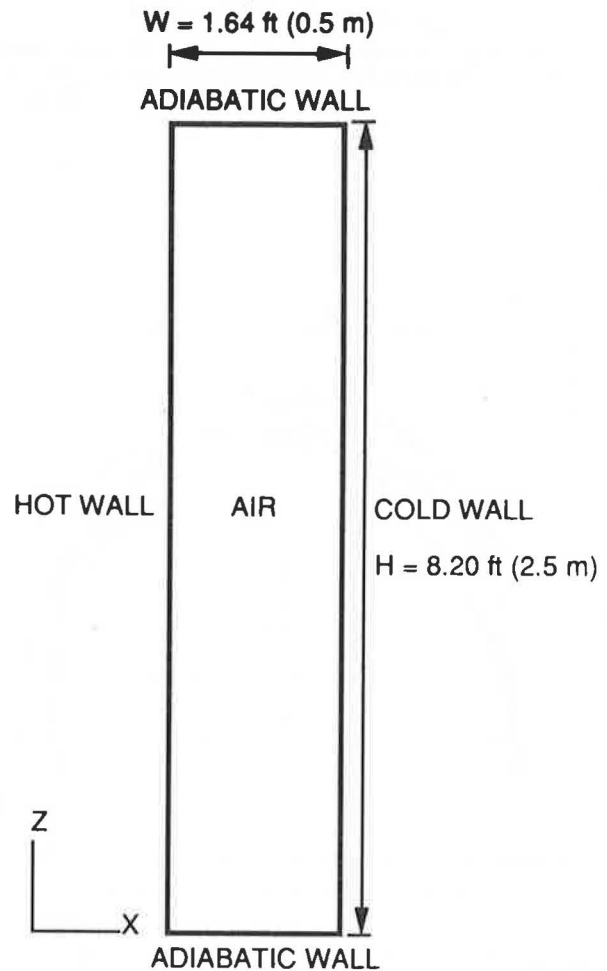


Figure 7 Sketch of the full-scale air-filled cavity

example, the difference between Cases 1 and 2 is $(5601 - 3578)/3578 = 56\%$. Unfortunately, no experimental data are available for the validation.

The previous discussion implies that the high- and low-Reynolds-number models may predict the same air temperature distributions in a room, but the convective heat transfer coefficients calculated are different. Since convective heat transfer coefficients are very important for space load calculation and the analysis of energy consumption in a room, further validation of the models is necessary.

Validation of the Model in a Full-Scale Air-Filled Cavity

The experiment used for validation was performed in a small-scale model. The resulting information is extrapolated to full scale by observing the similarity of Rayleigh number, which is the most important parameter in natural convection of indoor air flow. The small-scale cavity with water does not always accurately simulate a full-scale room with air. Important features are frequently distorted in the model test because of the difficulty of maintaining the similarity of Reynolds number and Prandtl number. Therefore, validation in a full-scale air-filled room was necessary for obtaining further confidence in the model, and that will be the subject of this section.

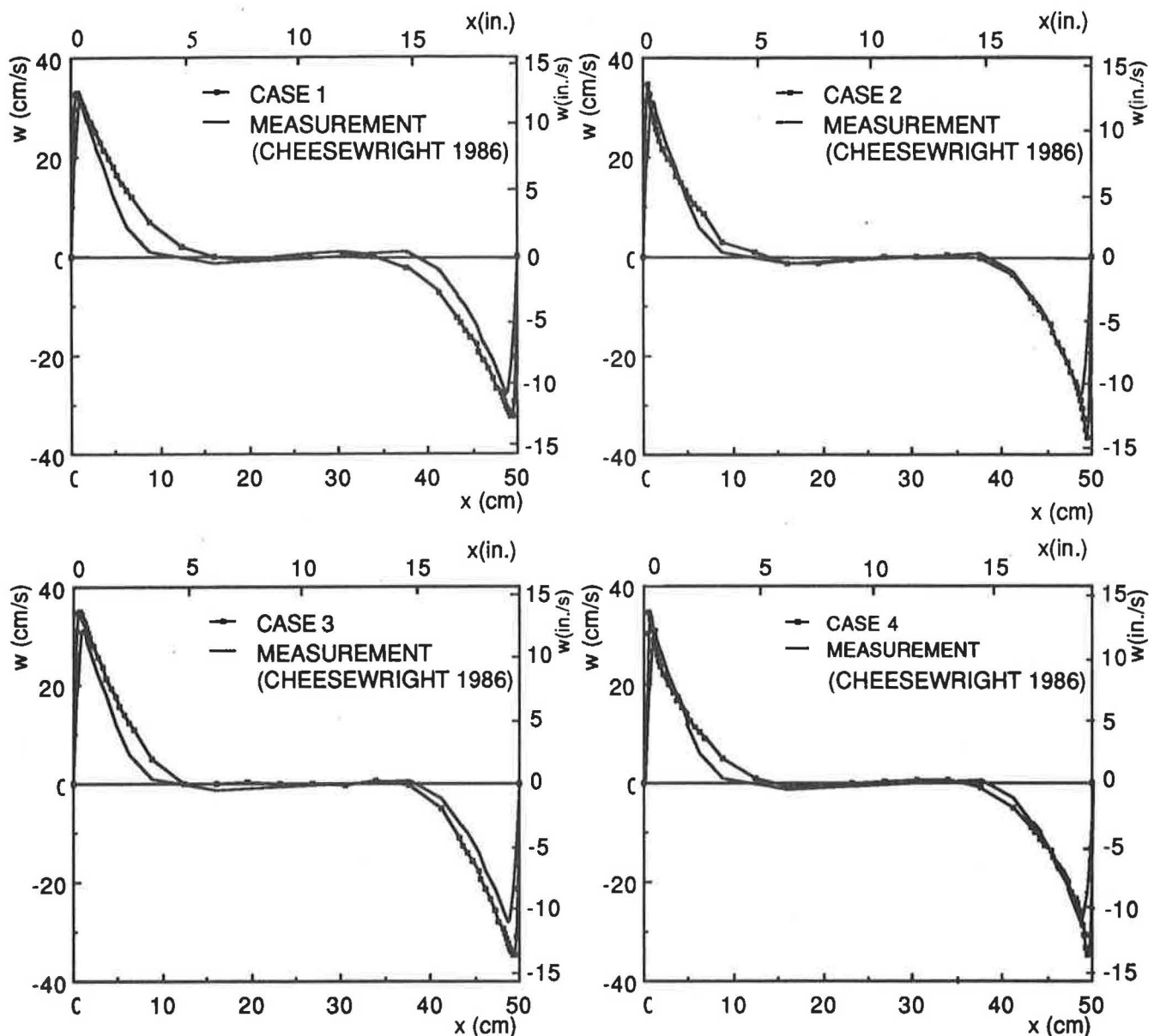


Figure 8 Profiles of vertical component of velocity in the middle height $z = 4.10$ ft (1.25 m)

The validation of the low-Reynolds-number $k-\epsilon$ model in a full-scale air-filled cavity was carried out by the application of the experimental results from Cheesewright et al. (1986). The air-filled cavity was designed with a height of 8.20 ft (2.5 m) and a width of 1.64 ft (0.5 m), as shown in Figure 7. The top and bottom walls were insulated to be adiabatic. The temperature difference between the hot wall and the cold wall was 82.4°F (45.8 K). The cold wall was cooled by the ambient air of the laboratory. The corresponding Rayleigh number is 5×10^{10} and is based on the cavity height. The air velocities and their fluctuations were measured by a laser-Doppler anemometer system.

Figure 8 shows the comparison between the measured velocity profiles at the middle height and the ones computed by the four models, as indicated in Table 1. The difference between the results predicted by the high-Reynolds-number $k-\epsilon$ model (Cases 1 and 3) and the low-Reynolds-number $k-\epsilon$ model (Cases 2 and 4) is smaller

than that in the water-filled cavity. However, it is clear that the results predicted by the low-Reynolds-number model (Cases 2 and 4) are in better agreement with the measurements. Figure 8 also indicates that the measured near-wall velocity profiles are not symmetric. Moreover, Cheesewright et al. (1986) also report that the velocity profile near the top wall is not the same as that near the bottom wall. The boundary layer at the bottom of the hot wall showed many of the characteristics of a laminar boundary layer (asymmetric relaminarization effects). In this study, these asymmetric effects may be attributed to the imperfect insulation of the roof of the cavity, since any heat loss in this region, even of a negligibly small proportion to the heat transfer across the cavity, could have a major effect (Cheesewright et al. 1986).

It should be noted that the asymmetric relaminarization effects also occurred in a case with a high level of insulation (Cowan et al. 1982). Cheesewright et al. (1986)

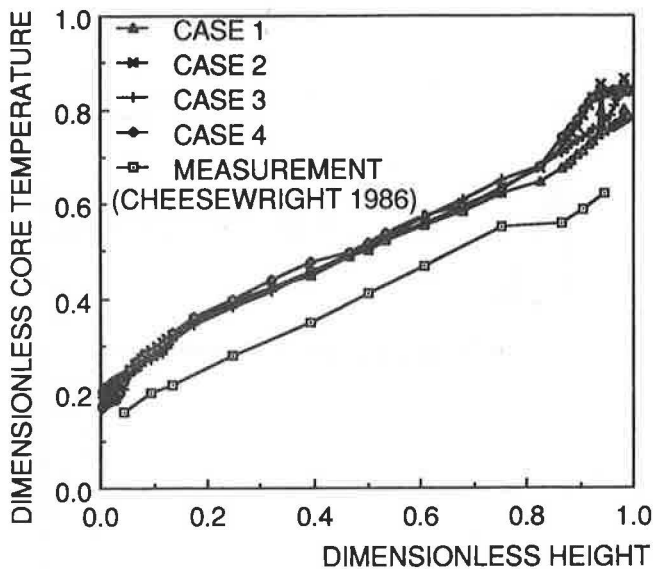


Figure 9 Vertical temperature profiles in the middle section $x = 9.84$ in. (25 cm)

proposed that there appears to be a feedback mechanism that not only enhances the sensitivity to heat loss through the roof but also seems to increase the strength of the flow across the roof and to reduce the strength of the flow across the floor. As a consequence, this will enhance the relaminarization at the bottom of the hot wall and increase the turbulence at the top of the cold wall such that the velocity profile in the middle height is asymmetric.

The vertical temperature profiles in the center section ($x = 9.84$ in. [0.25 m]) are given in Figure 9. The measured overall temperature of the cavity is lower than that of the computations. As we know, the variations of the physics properties of air are small within a temperature difference of 82.4°F (45.8 K). Therefore, the discrepancy is probably due to the imperfect insulation of the ceiling such that a certain amount of heat was transferred to the roof. As the final result, the overall air temperature of the cavity is lower than the mean temperature of the hot and cold walls.

Although the difference among the computed temperature profiles is small, as in the water-filled cavity, we have obtained large differences in the heat gains from the hot wall (or heat loss to the cold wall) among the computations. The heat gains for the four cases are 315 Btu/h·ft (303 W/m), 227 Btu/h·ft (219 W/m), 303 Btu/h·ft (291 W/m), and 226 Btu/h·ft (217 W/m), respectively. If a convective heat exchange coefficient is defined based on the wall-to-cavity-center temperature difference, its value for Case 1 is 0.93 Btu/ft²·h·°F (5.3 W/m²·K); for Case 2, 0.67 Btu/ft²·h·°F (3.8 W/m²·K); for Case 3, 0.90 Btu/ft²·h·°F (5.1 W/m²·K); and for Case 4, 0.67 Btu/ft²·h·°F (3.8 W/m²·K). The difference between the computations by the high-Reynolds-number model (Cases 1 and 3) and by the low-Reynolds-number model (Cases 2 and 4) is $(315-227)/227 \times 100\% = 39\%$.

In order to validate the models with respect to heat transfer, Figure 10 shows the relationship between the local Rayleigh numbers with the local Nusselt numbers. The local Rayleigh number (Ra_z) and local Nusselt number (Nu_z) in boundary flows are defined as:

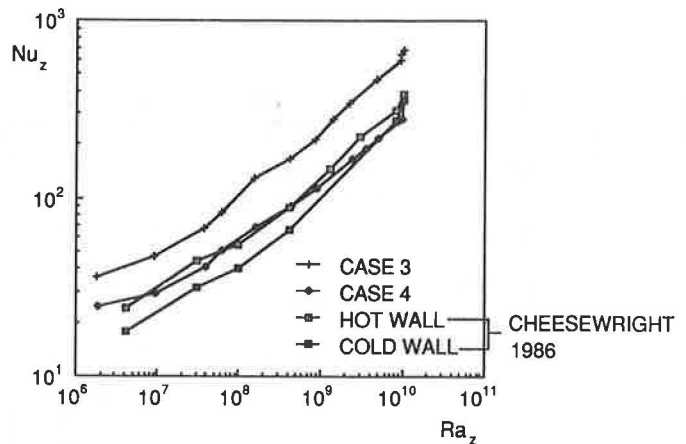


Figure 10 Local Nusselt number vs. local Rayleigh number

$$Ra_z = \frac{g\beta(T_h - T_o)z^3}{\nu a} \quad (13)$$

$$Nu_z = \frac{z(\partial T/\partial x)_{x=0}}{T_h - T_o} \quad (14)$$

Due to the insufficient thermal insulation of the top and bottom walls, asymmetrical data for the heat transfer through the hot and cold walls are found in the experiment by Cheesewright et al. (1986). Therefore, the measured data for both walls are given in Figure 10. It is clear that the computation with the low-Reynolds-number model is in good agreement with the measurement in the hot wall. The difference in heat transfer between the hot wall and the cold wall can be regarded as the heat loss through the top and bottom walls. We may conclude that the low-Reynolds-number model yields correct convective heat transfer coefficients and should be employed for the airflow computation in a room. In other words, the convective heat transfer coefficients calculated by the low-Reynolds-number model are reality and can be used for other purposes, such as space load calculation.

Chen (1988) reported that the high-Reynolds-number model with the wall functions presents a too-low convective heat exchange coefficient if the first grid is located outside the viscous sublayer of the boundary. In this study, a too-high convective heat exchange coefficient has been obtained when the first grid is in the viscous sublayer. This implies that the convective heat transfer computed by the high-Reynolds-number model depends on the first grid location. Therefore, this model is not suitable for the airflow simulation in a room from the viewpoint of the heat transfer in the boundary.

In the experiment, the velocity fluctuations at the middle height of the cavity are provided. However, no detailed information is given on the definition of the velocity fluctuations. If we assume that k is the square of the velocity fluctuation, a comparison of k profiles in the middle height of the cavity between the computations and the measurements can be done, as illustrated in Figure 11. The computations with the buoyancy production terms in the k and ϵ equations (Cases 3 and 4) are in very good agreement with the measurements in the middle section. In the near wall regions, the computations using the low-Reynolds-number k - ϵ model (Cases 2 and 4) present much better results.

Since the velocity fluctuation (turbulence energy) is one of the important parameters affecting comfort as

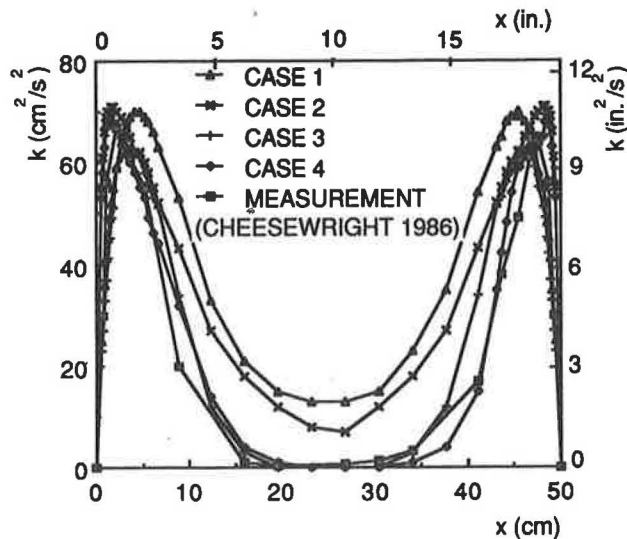


Figure 11 Profiles of kinetic energy of turbulence in the middle height $z = 4.10$ ft (1.25 m)

explored by Fanger et al. (1989), we may conclude from the above results that the model of Case 4 (low-Reynolds-number k - ϵ model with buoyancy production terms in the k and ϵ equations) will be the best for the prediction of natural-convection flow as well as mixed-convection flow in rooms.

CONCLUSIONS

A low-Reynolds-number k - ϵ model of turbulence developed by Lam and Bremhorst (1981) was first used to simulate the flow in a small-scale water-filled cavity with natural convection, for which detailed experimental data are available. The corresponding Rayleigh number (2.5×10^{10}) was as high as that encountered in a full-scale room with natural convection. The model was then applied to a full-scale air-filled cavity for further validation ($Ra = 5 \times 10^{10}$). The Boussinesq approximation was used for buoyancy and the buoyancy production terms in the k and ϵ equations were also studied.

From the validation in the water-filled cavity, it was found that near-wall velocity profiles calculated by the low-Reynolds-number k - ϵ model are in good agreement with the measurements despite peak values a little too high in the computations. The high-Reynolds-number k - ϵ model with wall functions (Launder and Spalding 1974) may result in an error as large as 61% in the near-wall velocity profile computations and 56% in the total heat gains from the hot wall. Although the error and the difference are smaller in the full-scale air-filled cavity, the validation supports the conclusions obtained from the results of the water-filled cavity. This implies that if the high-Reynolds-number model is applied for the airflow computation in a room, the predicted velocity field will deviate very much from experimental data.

The convective heat transfer computed by the high-Reynolds-number model depends on the first grid location. From the viewpoint of the heat transfer in the boundary, this model is not suitable for the airflow simulation in a room. In other words, the convective heat transfer coefficients calculated by the high-Reynolds-number model are not reality and cannot be used further.

The computations also show that the influence caused by the buoyancy production terms in the k and ϵ equations is small on the velocity and temperature profiles but is significant on the turbulence energy profiles. Accounting for the buoyancy production gives better turbulence energy distributions, which is very important because turbulence has a significant impact on the sensation of draft.

Hence, for the simulations of natural-convection flows as well as mixed-convection flows in rooms, it is better to use the low-Reynolds-number k - ϵ model of Lam and Bremhorst with the buoyancy production terms in the k and ϵ equations.

Since water is used as the medium in the small-scale cavity and water physics properties are assumed to be temperature-independent in the computations, a significant discrepancy between the computations and the experiment in temperature distribution was found due to this assumption. However, for natural- or mixed-convection flows in rooms, the assumption may be acceptable, because air physics properties are nearly independent of temperature.

ACKNOWLEDGMENTS

This investigation was financially supported by the Swiss Federal Office of Energy (BEW). The authors are indebted to Mr. C. Schönenberger at ETH-Zentrum for his preliminary work. Our thanks are also due to Mr. J.D. Parry of CHAM Ltd., London, for the help in the computer coding details.

NOMENCLATURE

a	= thermal diffusivity
A_μ, A_t, A_{C1}	= turbulence model constants
C_1, C_2, C_3, C_μ	= turbulence model constants
f_1, f_2, f_μ	= turbulence model functions
g_i	= gravity in i direction
H	= enthalpy
k	= kinetic energy of turbulence
l	= characteristic length scale in flow boundary
Nu_z	= local Nusselt number
Ra_z	= local Rayleigh number
R_k	= turbulence Reynolds number $(k^{3/2}y)/\nu_l$
R_m	= Reynolds number based on maximum velocity $(u_m y_m)/\nu_l$
R_t	= turbulence Reynolds number $(k^2)/\nu_l \epsilon$
S_k, S_ϵ	= source terms in k and ϵ equations due to buoyancy
T	= temperature
T_h	= hot wall surface temperature
T_o	= core temperature
u^+	= dimensionless velocity
V	= mean velocity
w	= velocity component in vertical (z) direction
x	= horizontal coordinate
x_i, x_j	= tensor notation for space coordinates
y	= smallest distance from a cell center to a wall
y^+	= dimensionless transverse coordinate
z	= vertical coordinate
β	= expansion coefficient
ϵ	= turbulence dissipation rate
μ	= fluid viscosity
ν	= kinetic viscosity
ρ	= density
σ_H	= diffusion Prandtl number for energy
σ_k	= diffusion Prandtl number for turbulence energy
σ_ϵ	= diffusion Prandtl number for dissipation rate

Subscripts

- l = laminar
- o = reference value
- t = turbulent

Superscripts

- ₉ = fluctuating component of the turbulence parameters

REFERENCES

- Anderson, D.A.; Tannehill, J.C.; and Pletcher, R.H. 1984. *Computational fluid mechanics and heat transfer*. New York: Hemisphere Publishing Corp.
- Betts, P.L., and Dafa'Alla, A.A. 1986. "Turbulent buoyant air flow in a tall rectangular cavity." *Significant Questions in Buoyancy Affected Enclosure or Cavity Flows*, ed: Humphrey, J.A.C., et al., pp. 83-91. New York: ASME.
- Buildings and Environment*. 1989. "Numerical solutions of fluid problems related to buildings, structures and the environment." Vol. 24, No. 1, pp. 3-110.
- Cheesewright, R.; King, K.J.; and Ziai, S. 1986. "Experimental data for the validation of computer codes for the prediction of two-dimensional buoyant cavity flows." *Significant Questions in Buoyancy Affected Enclosure or Cavity Flows*, ed: Humphrey, J.A.C., et al., pp. 75-81. New York: ASME.
- Chen, Q. 1988. "Indoor airflow, air quality and energy consumption of buildings." Ph.D. thesis, Delft University of Technology.
- Chen, Q.; van der Kooi, J.; and Meyers, A. 1988. "Measurements and computations of ventilation efficiency and temperature efficiency in a ventilated room." *Energy and Buildings*, Vol. 12, pp. 85-99.
- Chien, K.Y. 1982. "Predictions of channel and boundary-layer flows with a low-Reynolds number turbulence model." *AIAA Journal*, Vol. 20, No. 1, pp. 33-38.
- Cowan, G.H.; Lovegrove, P.C.; and Quarini, G.L. 1982. "Turbulent natural convection heat transfer in vertical single water-filled cavities." *Proceedings of the 7th International Heat Transfer Conference*, Paper NC13, Munich.
- Fanger, P.O.; Melikov, A.K.; Hanzawa, H.; and Ring, J. 1989. "Turbulence and draft: the turbulence of airflow has a significant impact on the sensation of draft." *ASHRAE Journal*, April, pp. 18-23.
- Hammond, G.P. 1982. "Profile analysis of heat/mass transfer across the plane wall-jet." *Proceedings of the 7th International Heat Transfer Conference*, Munich, Vol. 3, pp. 349-355.
- Hassid, S., and Poreh, M. 1978. "A turbulent energy dissipation model for flows with drag reduction." *Journal of Fluids Engineering, ASME Transactions*, Vol. 100, pp. 107-112.
- Heiss, A. 1987. "Numerische und experimentelle Untersuchungen der laminaren und turbulenten Konvektion in einem geschlossenen Behälter." Ph.D. thesis, Technische Universität Muenchen.
- Humphrey, J.A.C., and To, W.M. 1986. "Numerical simulation of buoyant, turbulent flow—ii. free and mixed convection in a heated cavity." *International Journal of Heat and Mass Transfer*, Vol. 29, No. 4, pp. 593-610.
- Kumar, K. 1983. "Mathematical modeling of natural convection in fire—a state of the art review of the field modeling of variable density turbulent flow." *Fire and Materials*, Vol. 7, No. 1, pp. 1-24.
- Lam, C.K.G., and Bremhorst, K. 1981. "A modified form of the $k-\epsilon$ model for predicting wall turbulence." *Journal of Fluids Engineering, ASME Transactions*, Vol. 103, pp. 456-460.
- Launder, B.E., and Sharma, B.I. 1974. "Application of the energy dissipation model of turbulence to the calculation of flow near a spinning disc." *Letters in Heat and Mass Transfer*, Vol. 1, pp. 131-138.
- Launder, B.E., and Spalding, D.B. 1974. "The numerical computation of turbulent flows." *Computer Methods in Applied Mechanics and Engineering*, Vol. 3, pp. 269-289.
- Murakami, S.; Kato, S.; and Suyama, Y. 1988. "Numerical and experimental study on turbulent diffusion fields in conventional flow type clean rooms." *ASHRAE Transactions*, Vol. 94, Part 2.
- Nielsen, P.V.; Restivo, A.; and Whitelaw, J.H. 1979. "Buoyancy-affected flows in ventilated rooms." *Numerical Heat Transfer*, Vol. 2, pp. 115-127.
- Parry, J.D. 1989. Private communications, CHAM Ltd., London.
- Patel, V.C.; Rodi, W.; and Scheuerer, G. 1985. "Turbulence models for near-wall and low Reynolds number flows: a review." *AIAA Journal*, Vol. 23, No. 9, pp. 1308-1319.
- Rosten, H.I., and Spalding, D.B. 1987. *The PHOENICE reference manual*, Version 1.4, Report No. TR200. London: CHAM Ltd.
- SAAH. 1987. *ROOMVENT 1987. Proceedings of the international conference on air distribution in ventilated spaces*, Vol. 3. Stockholm: Swedish Association of Air Handling Industries.
- Wilcox, D.C., and Rubesin, W.M. 1980. "Progress in turbulence modeling for complex flow fields including effects of compressibility." NASA Tech. Paper 1517.
- Whittle, G.E. 1986. "Computation of air movement and convective heat transfer within buildings." *International Journal of Ambient Energy*, Vol. 3, pp. 151-164.